Error evaluation in multi-rate sensor-based estimation systems including modelling errors and non-Gaussian noise (ISSFD)

Shunsuke Shimomura [(1)], Satoshi Ikari[(1)], Ryu Funase[(1)], Shin-ichi Nakasuka[(1)]

[(1)]The University of Tokyo
Tokyo, Japan
Email: nlab_info@space.t.u-tokyo.ac.jp

Abstract **–** Filtering algorithms using matrices such as the Kalman filter and the H∞ filter are powerful state estimators in discrete-time systems and have been applied and studied in a wide range of fields, including the space engineering field. Covariance analysis and norm analysis of transfer functions have been used to analytically predict the performance of these filters. However, to use these methods for feasibility verification of high-precision estimation in complex systems such as formation flights, some assumptions are the barrier; the time invariance system (both methods), only including Gaussian noise (covariance analysis), only applicable to single-rate sensors (transfer function norm analysis). Because of assumptions, it is difficult to evaluate the performance of the estimating system until conducting Monte Carlo simulations. In this study, we describe a method for analysing the error which processed in state estimation for a periodic time-varying linear system with multi-rate sensors, without using Monte Carlo simulations. Note that it is assumed that the filters and the system and the filter gains will converge to a steady state after a sufficient lapse of time, The system is subjected to uncertain disturbance during state transitions and observations. Disturbances are bounded and following a normal distribution. We introduce augmented state which the true state and estimation error are augmented together. Our method analyses both mean and covariance of augmented state. Mean analysis is expressed in the form of a transfer function. Analytical evaluation allows quantitative assessment of the impact on the control system when the estimation system is designed independently of the control system. The effect of periodic behaviour can be formulated as a time-delay system, and we show how to use this method to formulate the observed noise for a generalized plant in H∞ control theory. As a simple numerical example to demonstrate the practical applicability of the theory, we analysed the relative position estimation of two satellite formation flights and evaluate the effects of alignment error, attitude estimation error, and noise modelling error. Numerical simulations were also performed to validate the analytical results, showing that the evaluation method presented theoretically approximates the errors of the estimation system well.

.

I. INTRODUCTION

In spacecraft operations, state estimation plays a crucial role in achieving mission objectives. For the required control precision of a mission, sufficient estimation accuracy is necessary [1]. Therefore, during the design phase of a spacecraft system, determining the requirements for the state estimation system and verifying their feasibility is essential. This includes the selection of components and the design of filters. By iterating the design of filters and selection of sensors, and forecasting the performance of the estimation system, a feasible system solution that meets the requirements can be explored.

One of the mainstream methods for predicting the performance of estimation systems in recent years is Monte Carlo simulation. [2-5] This method evaluates the system's performance by statistically conducting enough numerical simulations to account for variations in conditions and noise. The ability to perform numerical calculations allows for the analysis of complex systems and non-Gaussian noise, which is a significant advantage.

On the other hand, covariance analysis, a method adopted even before the widespread use of computers, does not involve propagating state quantities but analytically determines the converging value of the filter's error covariance. [6,7] Since analytical calculations can be performed, it is possible to evaluate the performance of the estimation system with minimal computation. In the initial stages of consideration, it is also common to simply add up the expected error sources without using covariance analysis. In any case, from the perspective of computation time, this method is well-suited for iterations during the design stage.

Between Monte Carlo simulation and covariance analysis, there exists a trade-off between computational speed and accuracy. Monte Carlo simulation takes a considerable amount of time as it statistically evaluates performance through time-direction numerical simulations. In contrast, covariance analysis involves many constraints to solve analytically, making it challenging to model real-world problems. Furthermore, as spacecraft systems become more complex, such as in high-precision satellite formation flying systems, the importance of this trade-off increases due to the increased number of iterations required. Additionally, as the number of components and conditions handled in Monte Carlo simulations increases, the number of trials must also increase, while covariance analysis becomes more challenging to model.

In this paper, we propose an evaluation method that

possesses characteristics intermediate between Monte Carlo simulation and covariance analysis. The proposed method first calculates the filter gain and error covariance according to an assumed ideal operational scenario through simulation. It then evaluates the entire system incorporating the filter for the effects of disturbances and modelling errors using analytical methods such as the norm of the transfer function and covariance analysis. This method allows for determining the impact of factors such as sensor observation periods, alignment errors, and control inputs on estimation accuracy and requires only one time-direction simulation, thus reducing computational time.

Chapter 2 presents the mathematical derivation of the proposed method. In Section 1, we demonstrate under certain assumptions that filter gain and error covariance can be computed. Section 2 documents the derivation of a complete system representation, including the filter, using transfer function notation. In Section 3, utilizing the properties of the H_∞ norm, we derive Equation (37), which is the most crucial formula in this paper. This equation demonstrates how the drift component of the error can be calculated from power of the state, control inputs and disturbance, and H_∞ norms of modelling errors. Chapter 3 sets up a simple relative orbit estimation system and formulates both the proposed method and Monte Carlo simulations. Chapter 4 conducts analyses using both Monte Carlo simulations and the proposed method, demonstrating the validity of the proposed approach.

II. Mathematical Derivation of the Proposed Method

Section 1.

Calculation of Filter Gain and Error Covariance

In this study, we consider a discrete-time nonlinear system where the state at time k is denoted as $x_k \in \mathbb{R}^n$, the control input as $u_k \in \mathbb{R}^m$, and disturbances as $\omega_k \in \mathbb{R}^q$ This system can be described using nonlinear functions as follows:

$$x_{k+1} = f(x_k, u_k) + g(x_k)\omega_k \quad (1)$$

The observation equation, including observation noise $v_k \in \mathbb{R}^r$ and denoting the sensor index by i ($0 \le i \le N_i$), is given by:

$$z_k = h_i(x_k) + v_k \quad (2)$$

Note that ω_k and v_k are Gaussian noise with zero mean.

Furthermore, we denote the series of state and control inputs in an ideal scenario as x_k^* and u_k^* respectively. We place the following assumption:

Assumption 1:

x_k is sufficiently close to x_k^*, and in the neighbourhood of x_k^*, the variations of $\frac{\partial f}{\partial x}, \frac{\partial f}{\partial u}, \frac{\partial g}{\partial x}, \frac{\partial h_i}{\partial x}$ are small.

Under this assumption, by neglecting higher-order terms, Equations (1) and (2) can be approximated by a linear system as follows:

$$x_{k+1} \cong \left.\frac{\partial f}{\partial x}\right|_{x_k^*,u_k^*} x_k + \left.\frac{\partial f}{\partial u}\right|_{x_k^*,u_k^*} u_k + \left.\frac{\partial g}{\partial x}\right|_{x_k^*} \omega_k \quad (3)$$

$$z_k = \left.\frac{\partial h_i}{\partial x}\right|_{x_k^*} x_k + v_k \quad (4)$$

For simplicity, let us define:

$$A_k = \left.\frac{\partial f}{\partial x}\right|_{x_k^*,u_k^*}, \qquad B_k = \left.\frac{\partial f}{\partial u}\right|_{x_k^*,u_k^*}$$

$$G_k = \left.\frac{\partial g}{\partial x}\right|_{x_k^*}, \qquad H_{k,i} = \left.\frac{\partial h_i}{\partial x}\right|_{x_k^*}$$

When applying a Kalman filter to the system described by Equations (3) and (4), the filter gain $K_{k,i}$, and the propagation and update of the estimation error covariance P_k are as follows:

$$Q_k = \mathbb{E}[\omega_k \omega_k^T], \qquad R_{k,i} = \mathbb{E}\left[v_{k,i} v_{k,i}^T\right]$$

$$P_{k+1}^- = A_k P_{k,N_i}^+ A_k^T + G_k Q_k G_k^T \quad (5)$$

$$P_{k,0}^+ = P_k^- \quad (6)$$

$$K_{k,i} = S_{k,i} P_{k,i-1}^+ H_{k,i}^T \left(R_{k,i} + H_{k,i} P_{k,i-1}^+ H_{k,i}^T\right)^{-1} \quad (7)$$

$$P_{k,i}^+ = \left(I - K_{k,i}H_{k,i}\right)P_{k,i-1}^+\left(I - K_{k,i}H_{k,i}\right)^T + K_{k,i}R_{k,i}K_{k,i}^T \quad (8)$$

Where I is the identity matrix, P_k^- is the propagated estimation error covariance matrix after the disturbance, $P_{k,i}^+$ is the updated estimation error covariance matrix after observation by the i-th sensor, and $K_{k,i}$ is the filter gain for the i-th sensor. $S_{k,i}$ is a matrix that is an identity matrix when the i-th sensor can observe at time k and a zero matrix otherwise.

Assumption 2:

The system is a periodic time-varying system with a period N.

Under this assumption, we start with a sufficiently large positive definite matrix as the initial value for P_0^- and evolve P_k through Equations (5), (6), (7), and (8) until

$$P_{N\times l}^- = A_k P_{N\times l+N-1,N_i}^+ A_k^T + G_k Q_k G_k^T \quad (9)$$

holds. At convergence, the filter gain $K_{k,i}^*$ ($k = 0,1,\dots N-1$) and the estimated error covariance P_k^* ($k = 0,1,\dots N-1$) are established. As long as Assumptions 1 and 2 are valid, this estimation system will converge to a steady state where the filter gain and estimated error covariance remain constant at $K_{k,i}^*$ ($k = 0,1,\dots N-1$) and P_k^*($k = 0,1,\dots N-1$) respectively.

Hereinafter, for simplicity, let $k \coloneqq k \bmod N$.

Section 2.

Derivation of Transfer Function Representation for the System Including Filter

In the previous section, we derived a system formulation incorporating a Kalman filter. We define the system's coefficient matrix as $\tilde{X} = X + \Delta X$, where X is the original matrix and ΔX represents modelling errors. We

denote the estimated state as $\hat{x}$, and the error between the true state x and the estimate $\hat{x}$ as e. Additionally, we account for unknown disturbances $\tilde{\omega}_k$ and unknown observation noise $\tilde{v}_k$, both assumed to be energy-bounded signals. Under these conditions, the system with modeling errors and unknown disturbances, and the estimator in steady state, can be described as follows:

Propagation equation:

$$x_{k+1} = \tilde{A}x_k + \tilde{B}u_{k+1} + G\omega_{k+1} + \tilde{G}\tilde{\omega}_{k+1} \quad (10)$$

$$\hat{x}_{k+1}^{-} = A\hat{x}_{k,N_i}^{+} + Bu_{k+1} \quad (11)$$

$$e_{k+1}^{-} = Ae_{k,N_i}^{+} + \Delta Ax_k + \Delta Bu_{k+1} + G\omega_{k+1} + \tilde{G}\tilde{\omega}_{k+1} \quad (12)$$

Observation equation:

$$z_{k,i} = \tilde{H}_{k,i}x_k + v_{k,i} + \tilde{v}_{k,i} \quad (13)$$

$$z_{k,i} \cong H_{k,i}\hat{x}_{k,i-1}^{+} \quad (14)$$

$$\hat{x}_{k,0}^{+} = \hat{x}_k^{-} \quad (15)$$

$$\hat{x}_{k,i}^{+} = \hat{x}_{k,i-1}^{+} + K_{k,i}^{*}\left(z_{k,i} - H_{k,i}\hat{x}_{k,i-1}^{+}\right) \quad (16)$$

$$e_{k,i}^{+} = \left(I - K_{k,i}^{*}H_{k,i}\right)e_{k,i-1}^{+} - K_{k,i}^{*}\Delta H_{k,i}x_k - K_{k,i}^{*}v_{k,i} - K_{k,i}^{*}\tilde{v}_{k,i} \quad (17)$$

To describe the evolution of the estimation error e_{k,N_i}^{+} over one cycle, the equations (12) and (17) can be written down to form the following linear difference equation:

$$\begin{aligned} e_{k+N,N_i}^{+} &= Y_{k,0}e_{k,N_i}^{+} \\ &+ \sum_{n=0}^{N}\left\{\begin{matrix}\Phi_{k,n}\Delta A_{k+n} \\ +Y_{k,n+1}\sum_{i=0}^{N_i}\Psi_{k+n,i}\Delta H_{k+n,i}\end{matrix}\right\}x_{k+n} \\ &+ \sum_{n}^{N}\Phi_{k,n}\Delta B_{k+n}u_{k+n} \\ &+ \sum_{n}^{N}\Phi_{k,n}G_{k+n}\omega_{k+n} \\ &+ \sum_{n}^{N}\Phi_{k,n}\tilde{G}_{k+n}\tilde{\omega}_{k+n} \\ &- \sum_{n}^{N}\sum_{i=0}^{N_i}Y_{k,n+1}\Psi_{k+n,i}v_{k+n,i} \\ &- \sum_{n}^{N}\sum_{i=0}^{N_i}Y_{k,n+1}\Psi_{k+n,i}\tilde{v}_{k+n,i} \end{aligned} \quad (18)$$

Here, $X_{k,i_0}Y_{k,n_0}\Phi_{k,n}$, and $\Psi_{k,i}$ are defined as follows:

$$X_{k,i_0} = \prod_{i=i_0}^{N_i}\left(I - K_{k,i}^{*}H_{k,i}\right) \quad (19)$$

$$Y_{k,n_0} = \prod_{n=n_0}^{N}X_{k+n,0}A_{k+n} \quad (20)$$

$$\Phi_{k,n} = Y_{k,n+1}X_{k+n,0} \quad (21)$$

$$\Psi_{k,i} = X_{k,i+1}K_{k,i}^{*} \quad (22)$$

Equation (18) can be transformed into a transfer function representation using the Z-transform, by separating x_k and u_k into their nominal values x_k^*, u_k^*, and perturbation terms $\tilde{x}_k, \tilde{u}_k$, followed by converting from the discrete to the continuous frequency domain. The resulting expression is:

$$\begin{aligned} &\left(I - Y_{k,0}z^{-N}\right)e_k(z) \\ &= \sum_{n=0}^{N}\left\{\begin{matrix}\Phi_{k,n}\Delta A_{k+n} \\ +Y_{k,n+1}\sum_{i=0}^{N_i}\Psi_{k+n,i}\Delta H_{i,k+n}\end{matrix}\right\}\begin{pmatrix}z^{-N+n}\tilde{x}(z) \\ +x_{k+n}^{*}\end{pmatrix} \\ &+ \sum_{n}^{N}\Phi_{k,n}\Delta B_{k+n}\begin{pmatrix}z^{-N+n}\tilde{u}(z) \\ +u_{k+n}^{*}\end{pmatrix} \\ &+ \sum_{n}^{N}\Phi_{k,n}G_{k+n}z^{-N+n}\omega(z) \\ &+ \sum_{n}^{N}\Phi_{k,n}\tilde{G}_{k+n}z^{-N+n}\,\tilde{\omega}(z) \\ &- \sum_{i=0}^{N_i}\left(\sum_{n}^{N}Y_{k,n+1}\Psi_{k+n,i}z^{-N+n}\right)v_i(z) \\ &- \sum_{i=0}^{N_i}\left(\sum_{n}^{N}Y_{k,n+1}\Psi_{k+n,i}z^{-N+n}\right)\tilde{v}_i(z) \end{aligned} \quad (23)$$

Furthermore, by converting from the discrete frequency domain to the continuous frequency domain, we can rewrite Equation (23) as follows:

$$\begin{aligned} &\left(I - Y_{k,0}\mathrm{e}^{-sNT}\right)^{-1}e_k(s) \\ &= \left\{\begin{matrix} \sum_{n=0}^{N}U_x\begin{pmatrix}\mathrm{e}^{-s(N-n)T}\tilde{x}(s) \\ +x_{k+n}^{*}\end{pmatrix} \\ + \sum_{n}^{N}U_u\begin{pmatrix}\mathrm{e}^{-s(N-n)T}\tilde{u}(s) \\ +u_{k+n}^{*}\end{pmatrix} \\ + \sum_{n}^{N}U_\omega\omega_{k+n} \\ + \sum_{n}^{N}U_{\tilde{\omega}}\mathrm{e}^{-s(N-n)T}\,\tilde{\omega}(s) \\ - \sum_{i=0}^{N_i}\sum_{n}^{N}U_{v_i}\,v_i \\ - \sum_{i=0}^{N_i}\left(\sum_{n}^{N}U_{\tilde{v}_i}\mathrm{e}^{-s(N-n)T}\right)\tilde{v}_i(s) \end{matrix}\right\} \end{aligned} \quad (24)$$

Here, $U_x, U_u U_\omega U_{\tilde{\omega}} U_{v_i}$ and $U_{\tilde{v}_i}$ are defined as follows:

$$\left\{\begin{matrix} U_x = \Phi_{k,n}\Delta A_{k+n} + Y_{k,n+1}\sum_{i=0}^{N_i}\Psi_{k+n,i}\Delta H_{i,k+n} \\ U_u = \Phi_{k,n}\Delta B_{k+n} \\ U_\omega = \Phi_{k,n}G_{k+n} \\ U_{\tilde{\omega}} = \Phi_{k,n}\tilde{G}_{k+n} \\ U_{v_i} = Y_{k,n+1}\Psi_{k+n,i} \\ U_{\tilde{v}_i} = Y_{k,n+1}\Psi_{k+n,i} \end{matrix}\right. \quad (25)$$

Section 3.

Derivation of Error Power Norm

The input-output relationship of a system using the transfer function is denoted as:

$$Z(s) = G(s)W(s) \tag{26}$$

where $G(s)$ is the transfer function, and $W(s)$ and $Z(s)$ represent the Laplace transforms of the input $w(t)$, and output $z(t)$ respectively. The H_2 and H_∞ norms of $G(s)$ are defined as follows [8]:

$$\|G\|_2 = \left(\lim_{\alpha\to 0}\int_{-\infty}^{\infty} \mathrm{tr}\big(G(\alpha - j\omega)^T G(\alpha + j\omega)\big)\, d\omega\right)^{\frac{1}{2}} \tag{27}$$

$$\|G\|_\infty = \lim_{\alpha\to 0}\sup_{\omega} \bar{\sigma}\big(G(\alpha + j\omega)\big) \tag{28}$$

Here, $\bar{\sigma}(U)$ denotes the largest singular value of matrix U. The H_∞ norm, characterized by its subadditive property, is expressed as [8]:

$$\|F_1F_2\|_\infty \le \|F_1\|_\infty + \|F_2\|_\infty \tag{29}$$

It is known that the H_∞ norm of $G(s)$ is equivalent to the $G(s)$ norm mapping from $W(s)$ to $Z(s)$, leading to the following relationship [8]:

$$\|G\|_\infty = \sup_{W\in H_2\setminus\{0\}} \frac{\|Z\|_2}{\|W\|_2} = \sup_{W\in H_2\setminus\{0\}} \frac{\|GW\|_2}{\|W\|_2} \tag{30}$$

Thus, we have:

$$\|Z\|_2 \le \|G\|_\infty \|W\|_2 \tag{31}$$

Equation (30) further leads to the derivation of the submultiplicative property of the H_∞ norm:

$$\|F_1F_2\|_\infty \le \|F_1\|_\infty \|F_2\|_\infty \tag{32}$$

Moreover, since $W(s)$ and $Z(s)$ are the Laplace transforms of $w(t)$ and $w(t)$, by Parseval's theorem [9]:

$$\|W(s)\|_2 = \|w(t)\|_{\mathcal{L}2} \tag{33}$$

This implies:

$$\|z(t)\|_{\mathcal{L}2} \le \|G\|_\infty \|w(t)\|_{\mathcal{L}2} \tag{34}$$

Taking the time average of both sides in equation (34):

$$\mathrm{power}(z) \le \|G\|_\infty \cdot \mathrm{power}(w) \tag{35}$$

Where:

$$\mathrm{power}(w) \coloneqq \lim_{T\to\infty}\left(\frac{1}{T}\int_0^T |w(t)|^2 dt\right)^{\frac{1}{2}} \tag{36}$$

From equations (29), (32), and (35), equation (24) can be rewritten to estimate the magnitude of drift errors based on the power (mean values) of $x_k, u_k, \tilde{\omega}_k, \tilde{v}_{k,i}$ as follows:

$$\mathrm{power}(e) \le \left\|\left(I - Y_{k,0}e^{-sNT}\right)^{-1}\right\|_\infty \left\{\begin{array}{l} \sum_{n=0}^{N}\|U_x\|_\infty x_{k+n}^* \\ +\sum_{n=0}^{N}\left\|U_x e^{-s(N-n)T}\right\|_\infty \mathrm{power}(\tilde{x}) \\ +\sum_{n}^{N}\|U_u\|_\infty u_{k+n}^* \\ +\sum_{n}^{N}\left\|U_u e^{-s(N-n)T}\right\|_\infty \mathrm{power}(\tilde{u}) \\ +\sum_{n}^{N}\left\|U_{\tilde{\omega}} e^{-s(N-n)T}\right\|_\infty \mathrm{power}(\tilde{\omega}) \\ -\sum_{i=0}^{N_i}\left(\sum_{n}^{N}\left\|U_{\tilde{v}_i} e^{-s(N-n)T}\right\|_\infty\right)\mathrm{power}(\tilde{v}_i) \end{array}\right\} \tag{37}$$

Additionally, using the power spectral density (PSD) to describe the frequency domain of equation (36):

$$\int_{-\infty}^{\infty}\mathrm{PSD}_z\left(\frac{\omega}{2\pi}\right)d\omega \le \|G\|_\infty \int_{-\infty}^{\infty}\mathrm{PSD}_w\left(\frac{\omega}{2\pi}\right)d\omega \tag{38}$$

Thus, the error can also be estimated from the PSD, providing a comprehensive analysis of system stability and control.

III. Formulation of the Example Problem

Section 1. Proposed Method

To demonstrate the effectiveness of the proposed method, we established a simplified system for estimating the relative orbital motion of two satellites without actuators and conducted an analysis. The Local Vertical Local Horizontal (LVLH) coordinate system was employed to describe the relative orbital motion of the two satellites. The LVLH coordinate system is a non-inertial frame defined with the center of mass of a satellite on a certain orbit as the origin. It aligns the x-axis toward the center of the gravitational body from the satellite's center of mass, the z-axis in the direction of the satellite's orbital angular momentum vector, and the y-axis to form a right-hand system with the previously defined axes. Figure 1 illustrates the basis directions of the LVLH coordinate system.

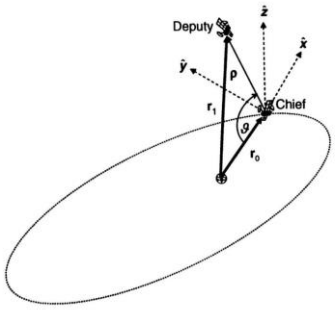

Figure 1: LVLH Coordinate System

The linearized equations for relative circular orbital motion, known as the HCW (Hill-Clohessy-Wiltshire) equations, were used to model the dynamics relative to the Chief satellite as follows[10]:

$$\begin{cases} \ddot{r}_x = 3\omega_z^2 r_x + 2\omega_z \dot{r}_y + a_x \\ \ddot{r}_y = 2n\dot{r}_x + a_y \\ \ddot{r}_z = -\omega_z^2 r_z + a_z \end{cases} \quad (39)$$

The initial position of the Deputy satellite was set as $r_x, r_y, r_z = \{0,10,0\}$. At this position, no acceleration due to dynamics occurs, so the nominal relative position remains constantly at $r_x^*, r_y^*, r_z^* = \{0,10,0\}$

The state variables are defined in the LVLH frame as the relative positions r_x, r_y, r_z and relative velocities r_x, r_y, r_z The values from the relative acceleration sensors a_x, a_y, a_z are used as inputs to the propagation equation, and the relative position and velocity are measured using position and velocity sensors. The propagation and observation equations can be expressed as follows:

Propagation Equation:

$$x_{k+1} = Ax_k + Bu_{k+1} + G\omega_{k+1}$$

$$\Leftrightarrow \begin{bmatrix} r_x \\ r_y \\ r_z \\ \dot{r}_x \\ \dot{r}_y \\ \dot{r}_z \end{bmatrix}_{k+1} = \begin{bmatrix} 1 & 0 & 0 & dt & 0 & 0 \\ 0 & 1 & 0 & 0 & dt & 0 \\ 0 & 0 & 1 & 0 & 0 & dt \\ 0 & 0 & 0 & 1 & 0 & 0 \\ 0 & 0 & 0 & 0 & 1 & 0 \\ 0 & 0 & 0 & 0 & 0 & 1 \end{bmatrix} \begin{bmatrix} r_x \\ r_y \\ r_z \\ \dot{r}_x \\ \dot{r}_y \\ \dot{r}_z \end{bmatrix}_k + \begin{bmatrix} \frac{dt^2}{2} & 0 & 0 \\ 0 & \frac{dt^2}{2} & 0 \\ 0 & 0 & \frac{dt^2}{2} \\ dt & 0 & 0 \\ 0 & dt & 0 \\ 0 & 0 & dt \end{bmatrix} \begin{bmatrix} a_x \\ a_y \\ a_z \end{bmatrix}_{k+1}$$

$$+ \begin{bmatrix} \frac{dt^2}{2} & 0 & 0 \\ 0 & \frac{dt^2}{2} & 0 \\ 0 & 0 & \frac{dt^2}{2} \\ dt & 0 & 0 \\ 0 & dt & 0 \\ 0 & 0 & dt \end{bmatrix} \begin{bmatrix} \omega_x \\ \omega_y \\ \omega_z \end{bmatrix}_{k+1} \quad (40)$$

Observation Equation:

$$z_{\dot{r}} = H_{\dot{r}} x_k + v_{k,\dot{r}}$$

$$\Leftrightarrow \begin{bmatrix} \dot{r}_{m,x} \\ \dot{r}_{m,y} \\ \dot{r}_{m,z} \end{bmatrix}_k = \begin{bmatrix} 0 & 0 & 0 & 1 & 0 & 0 \\ 0 & 0 & 0 & 0 & 1 & 0 \\ 0 & 0 & 0 & 0 & 0 & 1 \end{bmatrix} \begin{bmatrix} r_x \\ r_y \\ r_z \\ \dot{r}_x \\ \dot{r}_y \\ \dot{r}_z \end{bmatrix}_k + \begin{bmatrix} v_{\dot{x}} \\ v_{\dot{y}} \\ v_{\dot{z}} \end{bmatrix}_k \quad (41)$$

$$z_r = H_r x_k + v_{k,r}$$

$$\Leftrightarrow \begin{bmatrix} r_{m,x} \\ r_{m,y} \\ r_{m,z} \end{bmatrix}_k = \begin{bmatrix} 1 & 0 & 0 & 0 & 0 & 0 \\ 0 & 1 & 0 & 0 & 0 & 0 \\ 0 & 0 & 1 & 0 & 0 & 0 \end{bmatrix} \begin{bmatrix} r_x \\ r_y \\ r_z \\ \dot{r}_x \\ \dot{r}_y \\ \dot{r}_z \end{bmatrix}_k + \begin{bmatrix} v_x \\ v_y \\ v_z \end{bmatrix}_k \quad (42)$$

dt is the time step, $\dot{r}_{m,x}, \dot{r}_{m,y}, \dot{r}_{m,z}$ are the measured velocities, $r_{m,x}, r_{m,y}, r_{m.z}$ are the measured positions, $\omega_x, \omega_y, \omega_z$ represent the white noise in the accelerometer, $v_{\dot{x}}, v_{\dot{y}}, v_{\dot{z}}$ are the white noise in the velocity sensors, and v_x, v_y, v_z are the white noise in the position sensors. It is assumed that the velocity and position sensors have misalignment errors. Therefore, the nominal observation equations mentioned earlier actually contain model errors as follows:

$$\begin{aligned} z_{\dot{r}} &= \tilde{H}_{\dot{r}} x_k + v_{k,\dot{r}} \\ &= [R_{n_{\dot{r}}}(\theta_{\dot{r}}) \quad \mathbf{0}] x_k + v_{k,\dot{r}} \\ &= (H_{\dot{r}} + [R_{n_{\dot{r}}}(\theta_{\dot{r}}) - \boldsymbol{I} \quad \mathbf{0}]) x_k + v_{k,\dot{r}} \end{aligned} \quad (43)$$

$$\begin{aligned} z_r &= \tilde{H}_r x_k + v_{k,r} \\ &= [R_{n_r}(\theta_r) \quad \mathbf{0}] x_k + v_{k,r} \\ &= (H_r + [R_{n_r}(\theta_r) - \boldsymbol{I} \quad \mathbf{0}]) x_k + v_{k,r} \end{aligned} \quad (44)$$

Here, $R_n(\theta)$ is a 3D rotation matrix that rotates around axis n by angle θ.

When substituting equations (43) and (44) into equation (24) and taking the norm, the power of the error e can be estimated as follows:

$$\begin{aligned} \text{power}(e) \leq & \left\| \left(I - Y_{k,0} e^{-sNT}\right)^{-1} \right\|_\infty \\ & \times \sum_{n=0}^{N} \left\| Y_{k,n+1} \sum_{i=0}^{N_i} \Psi_{k+n,i} \right\|_\infty \Delta H_{i,k+n} x_{k+n}^* \\ = & \left\| \left(I - Y_{k,0} e^{-sNT}\right)^{-1} \right\|_\infty \\ \times & \sum_{n=0}^{N} \left\| Y_{k,n+1} \sum_{i=0}^{N_i} \Psi_{k+n,i} \right\|_\infty [R_{n_r}(\theta_r) - \boldsymbol{I} \quad \mathbf{0}] x_{k+n}^* \end{aligned}$$

$$= \left\| \left(I - Y_{k,0} e^{-sNT}\right)^{-1} \right\|_{\infty} \times \sum_{n=0}^{N} \sum_{i=0}^{N_i} \left(\begin{matrix} \left\| Y_{k,n+1} \Psi_{k+n,i} \right\|_{\infty} \\ \times \left\| R_{n_r}(\theta_r) \right\|_{\infty} \end{matrix} \right) \text{power} \left(\begin{bmatrix} r_x^* \\ r_y^* \\ r_z^* \end{bmatrix} \right) \quad (45)$$

The settings for each value are summarized in Table 1:

Table 1: Computational Parameters

	symbol	value
Time step	dt	0.1 $[s]$
Accelerometer Noise	$\omega_x^2, \omega_y^2, \omega_z^2$	0.3 $[(m/s^2)^2]$
Velocity Sensor Noise	v_x^2, v_y^2, v_z^2	0.2 $[(m/s)^2]$
Velocity Measurement Interval	$-$	0.3 $[s]$
Velocity Sensor misalignment	$\theta_{\dot{r}}$	1 $[deg]$
Position Sensor Noise	v_x^2, v_y^2, v_z^2	0.1 $[m^2]$
Position Measurement Interval	$-$	1 $[s]$
Position Sensor misalignment	θ_r	1 $[deg]$

Section 2. Monte Carlo simulation

At the start of each trial, the alignment tilt directions of the position and velocity sensors are determined randomly. Subsequently, numerical simulations are conducted over enough time steps. Statistics are collected per orbital period to calculate the mean and variance of the errors. The number of trials was set to 60, with each trial running for 1000 steps.

IV. RESULTS

We compare the estimates of error mean and variance obtained through the proposed method with the results from Monte Carlo simulations. Figure 2 displays a graph with the x-axis showing the intra-orbital period time and the y-axis showing the standard deviation of the position estimation error in the x-axis direction. The black line indicates the results from each trial of the Monte Carlo simulation, while the red line represents the outcomes derived from the covariance analysis within the proposed method. Figure 3 illustrates the results of the analysis using the H_∞ norm, with the y-axis representing the power of the position estimation error and the x-axis showing the intra-orbital period time. Figure 4 shows the standard deviation of the position estimation error in the x-axis direction for the case without misalignment, formatted similarly. In both Figures 3 and 4, the black line represents the Monte Carlo simulations, and the red line shows the power of the position estimation error determined through the norm analysis of the proposed method.

As indicated in Figures 2, 3, and 4, the results of the proposed method effectively capture the graphical shape of the results obtained from the simulations. This capability to analytically determine the behaviour when combining sensors operating at multiple rates is a strength of this method.

In Figure 2, the results of the covariance analysis, which show the variation of the estimates, are observed to estimate lower errors compared to the simulation. This lower estimation is due to the covariance analysis not accounting for the impact of unknown disturbances or modelling errors. Indeed, by examining Figure 4, which compares the simulation results without misalignment, the estimation of error variance has been successful.

In Figure 3, the fact that the calculated results of the error mean by the proposed method cover almost all trials of the simulation aligns well with the outcome expected from Equation (36), where the inequality is used to calculate the worst-case scenario. This consistency suggests that evaluating the system with the H_∞ norm is beneficial and indicative of the utility of the H_∞ norm for system evaluation.

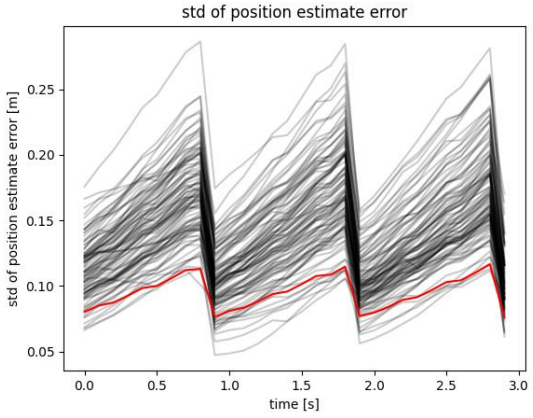

Figure 2: std of x-axis position estimate error. (black: Monte Carlo, red: Proposed method)

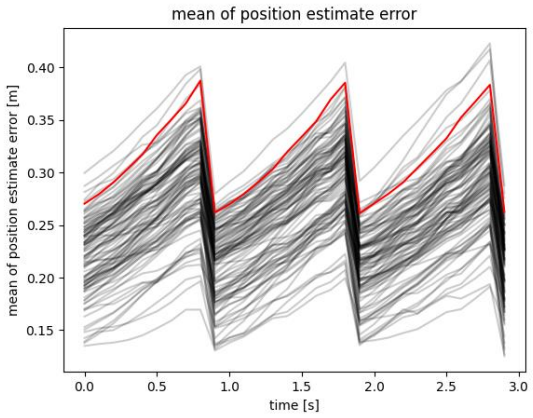

Figure 3: mean of position estimate error.
(black: Monte Carlo, red: Proposed method)

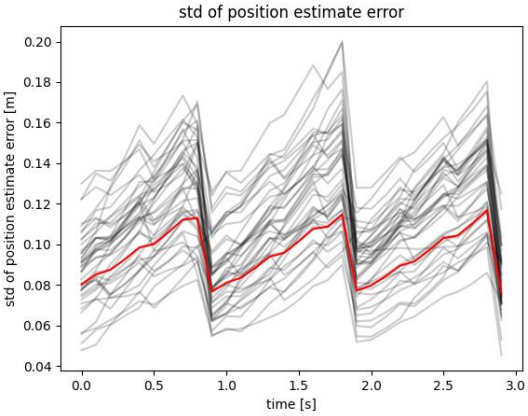

Figure 4: std of x-axis position estimate error without misalignment.
(black: Monte Carlo, red: Proposed method)

V. CONCLUSION

In this paper, we proposed a novel method for evaluating estimation systems. The method we introduced can perform analyses faster than Monte Carlo simulations and more faithfully to the model than covariance analysis. This mathematically derived approach has been applied to settings involving multi-rate sensors and sensor misalignment, providing estimates of estimation accuracy. Particularly for the power of estimation errors, this method, which calculates worst-case values using the H_∞ norm, demonstrated remarkable predictive accuracy.

VI. REFERENCES

Examples:

[1] Matsuka, Kai, Daniel Scharf, Nuno Filipe, Carl Seubert, and David Bayard. "Relative sensing, control precision, and mission delta-v trade-offs for precision formation flying in planetary orbit." Journal of Guidance, Control, and Dynamics vol. 42, no. 5: pp. 992-1006, 2019.

[2] Ramos, J. Humberto, Kevin M. Brink, Prashant Ganesh, and John E. Hurtado. "Factorized partial-update Schmidt–Kalman filter." Journal of Guidance, Control, and Dynamics vol. 45, no. 9 pp. 1567-1582, 2022.

[3] Brink, Kevin M. "Partial-update schmidt–kalman filter." Journal of Guidance, Control, and Dynamics vol. 40(9). pp. 2214-2228, 2017.

[4] Zheng, S., Jiang, L., Yang, Q., Zhao, Y., & Wang, Z. Adaptive PHD Filter with RCS and Doppler Feature for Space Targets Tracking via Space-Based Radar. IEEE Transactions on Aerospace and Electronic Systems, 2023.

[5] Sabatini, M., & Palmerini, G. B. Filtering Strategies for Relative Navigation in Lunar Scenarios Using LCNS. Aerospace, 11(1), 59, 2024.

[6] Markley, F. L. Analytic Steady-State Accuracy of a Three-Axis Spacecraft Attitude Estimator. Journal of Guidance, Control, and Dynamics, vol. 40(9), pp. 2399-2400, 2017

[7] de Mijolla, L., Cavrois, B., Profizi, A., Renault, C., & Cropp, A. Covariance analysis tool for far non-cooperative rendezvous. In AIAA Guidance, Navigation, and Control (GNC) Conference (p. 5118). 2013.

[8] G. Zames, "Feedback and optimal sensitivity: Model reference transformations weighted seminorms and approximate inverses", Proc. 17th Allerton Conf., pp. 744-752, 1979.

[9] Parseval des Chênes, Marc-Antoine "Mémoire sur les séries et sur l'intégration complète d'une équation aux differences partielle linéaire du second ordre, à coefficiens constans" presented before the Académie des Sciences (Paris) on 5 April 1799. This article was published in Mémoires présentés à l'Institut des Sciences, Lettres et Arts, par divers savans, et lus dans ses assemblées. Sciences, mathématiques et physiques. (Savans étrangers.), vol. 1, pages 638-648 (1806).

[10] W. H. CLOHESSY and R. S. WILTSHIRE. "Terminal guidance system for satellite rendezvous," Journal of the Aerospace Sciences, vol. 27(9), pp. 653–658, 1960.